

# Status of $e^+e^- \rightarrow \pi^+\pi^-$ analysis with SND at VEPP-2000

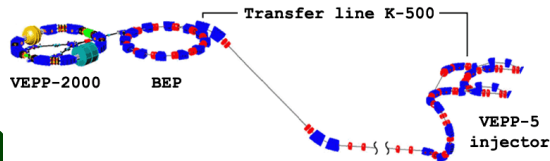
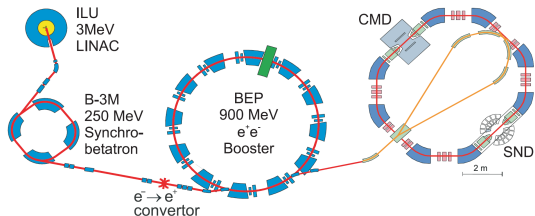
Kupich A.  
on behalf of SND collaboration

Muon g-2 Theory Initiative workshop  
September 8 – 12, 2025





# VEPP-2000 $e^+e^-$ collider



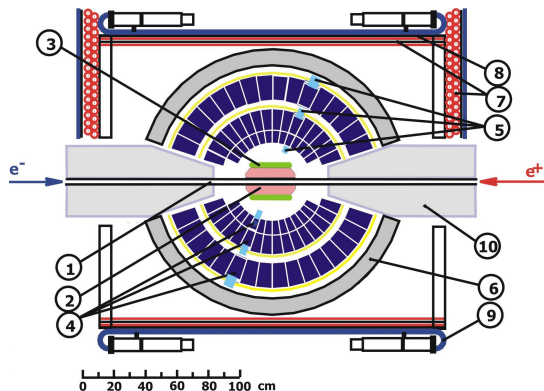
## VEPP-2000 parameters

- c.m. energy  $E=0.3\text{-}2.0$  GeV
- Luminosity at  $E=1.8$  GeV  
 $10^{32} \text{cm}^{-2} \text{sec}^{-1}$  (project)  
 $6 \times 10^{31} \text{cm}^{-2} \text{sec}^{-1}$  (achieved)
- Beam energy spread - 0.6 MeV at  $E=1.8$  GeV

- 10 times more intense positron source
- Experiments at upgraded VEPP-2000 were continued in the late 2016







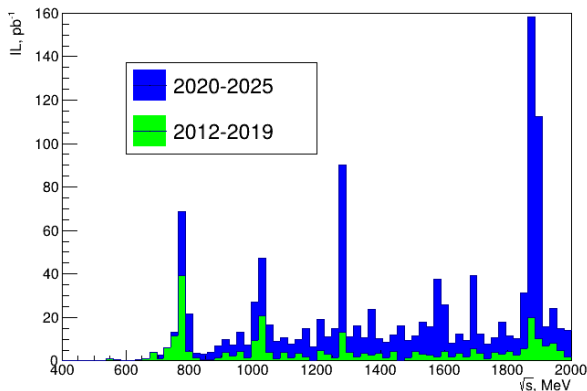
1-beam pipe, 2-tracking system, 3- aerogel Cherenkov counter , 4 - Nal(Tl) crystals, 5 - phototriodes, 6 - iron muon absorber, 7-9 - muon detector, 10 - focusing solenoids.

Main physics task of SND is study of all possible processes of  $e^+e^-$  annihilation into hadrons below 2 GeV

- The total hadronic cross section, which is calculated as a sum of exclusive cross sections
- Study of hadronization (dynamics of exclusive processes)
- Study of the light vector mesons
- Production of the C-even resonances







Current  $e^+e^- \rightarrow \pi^+\pi^-$  analysis is based on the statistics, collected in **2017 – 2018** in 100 energy points  $\sqrt{s} < 1$  GeV. In recent years  $900 \text{ pb}^{-1}$  data are collected in the  $\sqrt{s} \approx M_\omega$  and  $M_\omega < \sqrt{s} < 2$  GeV energy regions. With 1.1 and 3.9 times greater statistics.

## Timeline

MHAD2012 –  $48 \text{ pb}^{-1}$   
 RHO 2013 –  $32 \text{ pb}^{-1}$   
 MHAD2017 –  $50 \text{ pb}^{-1}$   
**RHO 2018 –  $90 \text{ pb}^{-1}$**   
 MHAD2019 –  $65 \text{ pb}^{-1}$   
 RHO 2019 –  $1 \text{ pb}^{-1}$   
 MHAD2020 –  $45 \text{ pb}^{-1}$   
 MHAD2021 –  $57 \text{ pb}^{-1}$   
 MHAD2022 –  $360 \text{ pb}^{-1}$   
 MHAD2023 –  $223 \text{ pb}^{-1}$   
 MHAD2024 –  $114 \text{ pb}^{-1}$   
 PHI 2024 –  $57 \text{ pb}^{-1}$   
 RHO 2024 –  $33 \text{ pb}^{-1}$   
 OMEG2024 –  $48 \text{ pb}^{-1}$



- 1  $N_{ch} \geq 2$  – two or more charged particles are allowed
- 2  $|\Delta\theta| = |180^\circ - (\theta_1 + \theta_2)| < 14^\circ$  and  $|\Delta\varphi| = |180^\circ - |\varphi_1 - \varphi_2|| < 6^\circ$
- 3  $E_{1,2} > 40$  MeV, here  $E_i$  – energy deposition for the  $i$ -th particle
- 4  $60^\circ < \theta_0 = (\theta_1 - \theta_2 + 180^\circ) \times 0.5 < 120^\circ$
- 5  $|r_1| < 1$  cm ,  $|r_2| < 1$  cm, here  $r_i$  – distance between a track of  $i$ -th particle and the beam axis
- 6  $|z_{01}| < 8$  cm ,  $|z_{02}| < 8$  cm, here  $z_i$  – longitudinal coordinate of the vertex
- 7 Cosmic veto:  $veto = 0$  ( $\sqrt{s} < 900$  MeV)

With  $e^+e^- \rightarrow \pi^+\pi^-$ ,  $e^+e^- \rightarrow \mu^+\mu^-$ ,  $e^+e^- \rightarrow e^+e^-$  and residual cosmic background events passing these cuts. Contributions from  $e^+e^- \rightarrow e^+e^-e^+e^-$  (0.2 – 3.5 %) and  $e^+e^- \rightarrow \pi^+\pi^-\pi^0$  (0.01 – 0.6 %) to  $e^+e^- \rightarrow \pi^+\pi^-$  were estimated from MC and Data samples. Efficiencies for major processes are calculated via MC simulation with BABAYAGA-NLO used for primary particles generation.





In order to separate events with  $e^+e^-$  and  $\pi^+\pi^-$  in the final state machine learning methods (based on BDTG) were developed, with input parameters:

- $^0e_j$  – energy deposition for the  $j$ –th layer in the central tower
- $^1e_j$  – energy deposition for the  $j$ –th layer in the towers, next to the central one
- $^2e_j$  – energy deposition for the  $j$ –th layer outside
- $E_j$  – full energy deposition for  $j$ –th layer
- $E$  – total energy deposition
- $^0e$  – energy deposition in the central tower
- $^1e$  – energy deposition in the towers, next to the central one
- $^2e$  – residual energy deposition
- $\sum_{j=1}^3 E_j R_j / E$  – longitudinal cluster size
- $\sum_{k=1}^2 {}^k e A_k / E$  – transversal cluster size ( $A_{1,2} = 9^\circ, 18^\circ$ )

Overall  $(4 \times 3 + 3 + 2 + 1) \times 2 = \mathbf{36}$  parameters for the main discriminator.

There is a version of discriminator for separate particles.

And one for  $\mu/\pi$  separation





# Changes in the $e^+e^- \rightarrow e^+e^-e^+e^-$ subtraction

- The new version of the subtraction algorithm is mostly data-driven
- Number of  $e^+e^- \rightarrow e^+e^-e^+e^-$  events passing collinear cuts is derived from special sample of events: noncollinear events with two ACC firing and total energy deposition in the EMC less than  $0.25\sqrt{s}$
- Ratio is mostly derived from the Data (except for efficiency of the  $E_{tot} < 0.25\sqrt{s}$  cut)
- The new technique provides greater number of the background events in the  $\sqrt{s} > 0.9$  GeV region





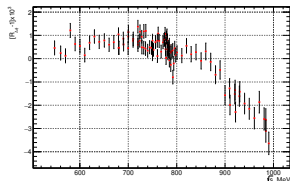
# Pion loss due to the nuclear interactions

- Probability of the pion loss in Data is derived from the  $e^+e^- \rightarrow \pi^+\pi^-\pi^0$  events with one charged particle detected
- Energies of charged pions and direction of undetected particle are calculated under assumption of the total energy and momentum conservation
- Contribution of events with poorly reconstructed tracks is excluded by limiting number of hits in the region of the DC, corresponding to the direction of missing pion
- For the  $e^+e^- \rightarrow \phi \rightarrow \pi^+\pi^-\pi^0$  events there is a contribution from  $e^+e^- \rightarrow \phi \rightarrow K^+K^-$ . To limit it  $dE/dx$  cuts are implemented. Residual background estimated from a fit of the distance between a track and the beam axis distribution
- Overall correction (for two pions) is energy independent for  $\sqrt{s} > 0.5$  GeV and equal to 0.9935

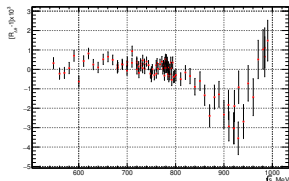




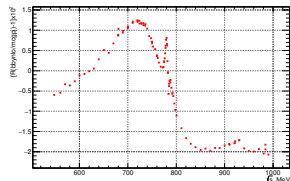
A new version (with  $e^+e^- \rightarrow \pi^+\pi^-$ ) of the **BabaYaga-NLO** is implemented. It's considered preliminary due to lack of ISR processes. Comparison with **MCGPJ** shows noticeable difference in the  $\sqrt{s} > 800$  MeV region for  $e^+e^- \rightarrow \pi^+\pi^-$ .



The  $\Delta\phi$  cuts efficiency changes



Ones for the  $\Delta\theta$  cuts



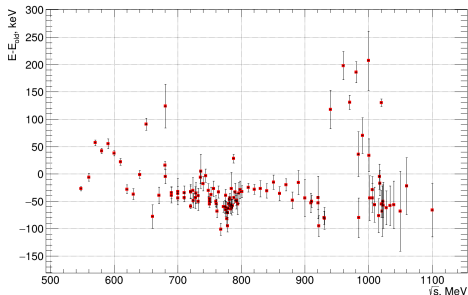
Shifts in radiative corrections



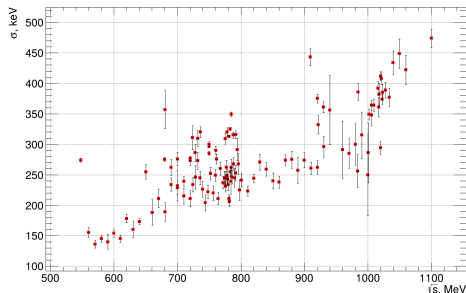


# New energy measurements

Reanalysis of the recorded Compton spectrums was performed. Weighted measurements are used, each one is proportional to the number of  $e^+e^- \rightarrow e^+e^-$  events. Contributions of bad runs, excluded from the analysis, are removed from average.



Deviation from old measurements

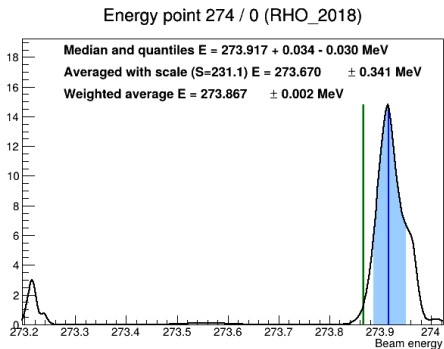


c.m. energy spread

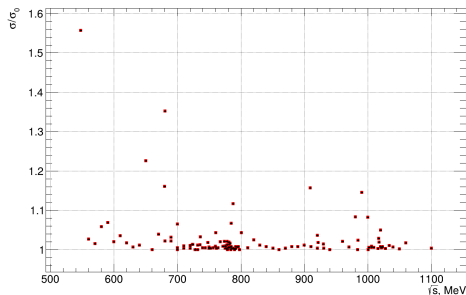




Drift of the mean c.m.e. can contribute to the energy spread. It's negligible for all but 7 energy points.



Energy distribution for  $E_{beam} = 274.0$  MeV.



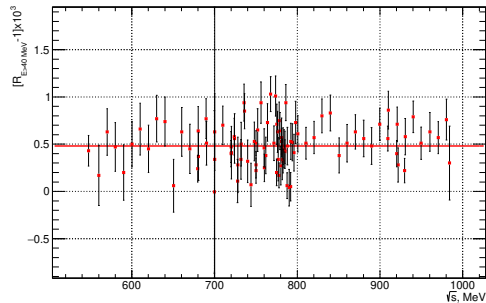
Boost of the c.m. energy spread



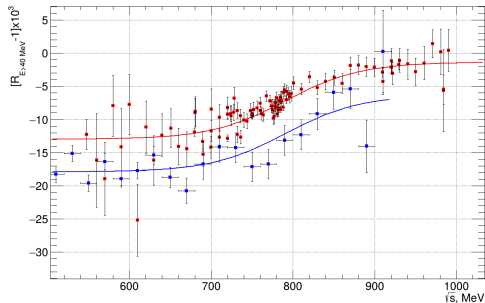


# Efficiency of the $E_i > 40$ MeV cut

Using  $ee$ ,  $2\pi$  and  $3\pi$  events (with some additional cuts\*) to calculate efficiency corrections



$e^+e^- \rightarrow e^+e^-$  events



$e^+e^- \rightarrow \pi^+\pi^-$  events

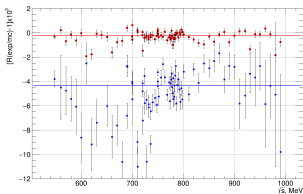
The largest correction comes from  $E_i > 40$  MeV cut. There is 0.5 % difference between corrections derived from  $e^+e^- \rightarrow 2\pi$  and  $e^+e^- \rightarrow 3\pi$  events.



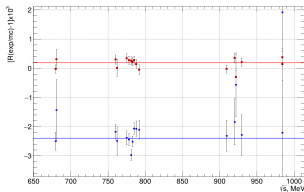
\* ACC (not)firing, muon suppression,  $E_{max} > 160$  MeV



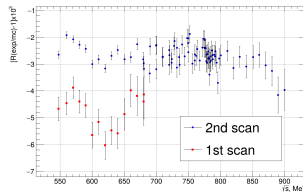
Using  $ee$  and  $2\pi$  pseudo-events to calculate efficiency correction.



Corrections for **electrons** and **pions** for the 1-st scan.



Corrections for **electrons** and **pions** for the 2-nd scan.



Corrections for pions in pseudo-events from  $e^+e^- \rightarrow 3\pi$  for the **first** and **second** scans

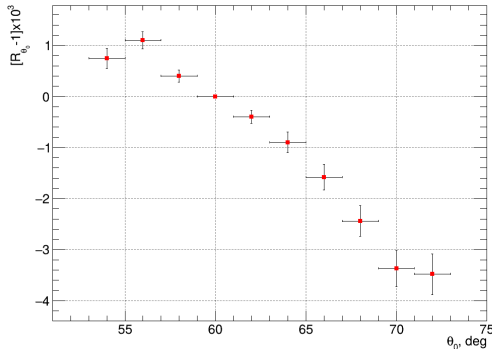
For  $e^+e^- \rightarrow e^+e^-$  events correction is  $< 0.1\%$ . For  $e^+e^- \rightarrow \pi^+\pi^-$  they are  $0.24\%$  and  $0.42\%$  for first and second scans. Corrections for pions in pseudo-events from  $e^+e^- \rightarrow 3\pi$  are in agreement with ones from  $e^+e^- \rightarrow \pi^+\pi^-$ .





# Contribution from $\theta_0$ cut

Variation of  $\theta_0$  cut results in changes of the cross section measurement results. They show no energy dependence. Averaged shifts of cross sections for different  $\theta_0$  cuts are:



## Systematics $\theta_0$ :

- Improvements of the reconstruction algorithm are followed by reduction of discrepancy between MC and Data
- Deviation from unity is in  $10^{-3}$  to  $-3.5 \times 10^{-3}$  range
- Contribution of the  $60^\circ < \theta_0 < 120^\circ$  cut to the systematic uncertainty is **0.4 %**

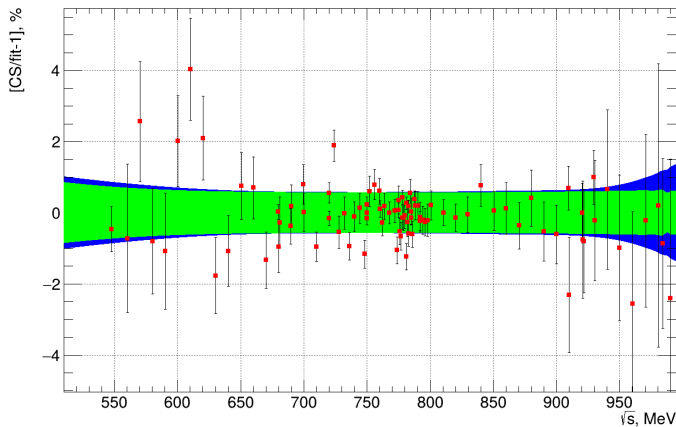




Source	$\sqrt{s} < 700 \text{ MeV}, \%$	$\sqrt{s} > 700 \text{ MeV}, \%$
$e/\pi$	0.2	0.1
$E_i > 40 \text{ MeV}$	<b>0.5</b>	
rad	0.1	
nc2	0.1	
col	0.2	
$\theta_0$	<b>0.4</b>	
nucl	0.1	
total	0.72	0.7





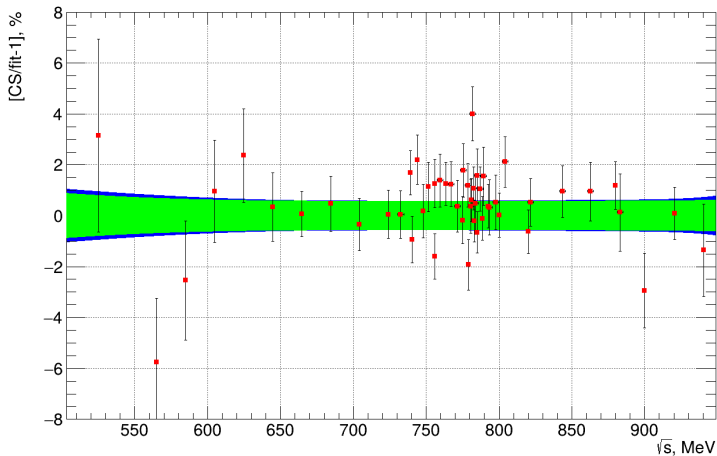


Fit results:  $M_\rho = 775.56 \pm 0.16$  MeV,  $\Gamma_\rho = 149.69 \pm 0.33$  MeV,  
 $M_\omega = 782.36 \pm 0.06$  MeV,  $\Gamma_\omega = 8.723 \pm 0.07$  MeV,  
 $Br_{\omega \rightarrow 2\pi} = 1.67 \pm 0.023$  %,  $\varphi_{\rho\omega} = 0.131 \pm 0.01$ ,  $\chi^2/\text{n.d.f.} = 1.7$





# Comparison with 2013 data (UNBLINDED)



Deviation 2013 measurements from our fit, green area – systematics,  
blue onw - total uncertainty





# Selecting 2019 data

- ❶  $N_{ch} \geq 2$  – two or more charged particles are allowed
- ❷  $|\Delta\theta| = |180^\circ - (\theta_1 + \theta_2)| < 14^\circ$  and  $|\Delta\varphi| = |180^\circ - |\varphi_1 - \varphi_2|| < 6^\circ$
- ❸  $E_{1,2} > 40$  MeV, here  $E_i$  – energy deposition for the  $i$ -th particle
- ❹  $60^\circ < \theta_0 = (\theta_1 - \theta_2 + 180^\circ) \times 0.5 < 120^\circ$
- ❺  $|r_1| < 1$  cm ,  $|r_2| < 1$  cm, here  $r_i$  – distance between a track of  $i$ -th particle and the beam axis
- ❻  $|z_{01}| < 8$  cm ,  $|z_{02}| < 8$  cm, here  $z_i$  – longitudinal coordinate of the vertex
- ❼ Cosmic veto:  $veto = 0$
- ❽  $R_{1,2}^{acc} = 1$  – both particles pass through ACC
- ❾ Event ID:
  - $e^+e^- \rightarrow e^+e^-$ : both particles caused ACC firing,  $R_{1,2}^{BDT} > 0.8$
  - $e^+e^- \rightarrow \pi^+\pi^-$ : both particles failed to fire ACC,  $R_{1,2}^{BDT} < 0.8$





Source	$\sqrt{s} < 580 \text{ MeV}, \%$	$\sqrt{s} \geq 580 \text{ MeV}, \%$
act	1.0	1.4
$\mu$	0.4	0.2
$E_i > 40 \text{ MeV}$	0.5	
BDT	0.3	
region	1.0	
rad	0.1	
nc2	0.1	
col	0.3	
$\theta_0$	0.4	
nucl	0.2	
total	1.7	1.9

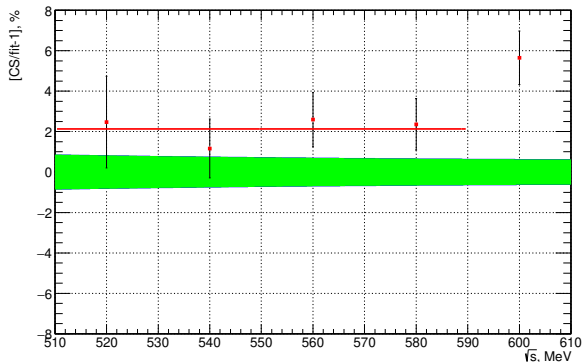
Measurement suffers from the low statistics, resulting in high statistical uncertainties for the calculated corrections.





# Comparison with 2019 data (UNBLINDED)

Comparison with fit of the 2018 data shows  $2.1 \pm 1.9$  % shift.

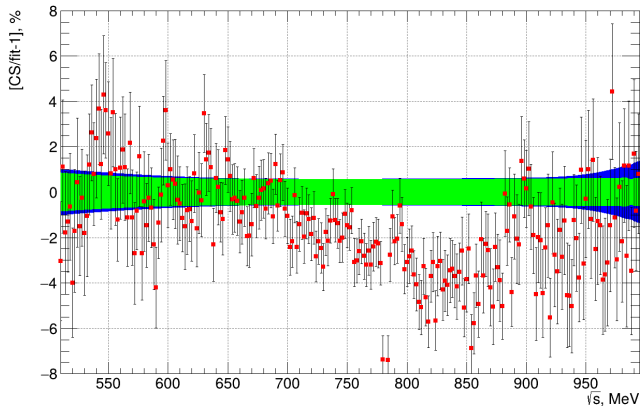


Deviation of alternative 2019 measurements from our fit, green area – systematics, blue one - total uncertainty





# Comparison with BaBar (UNBLINDED)



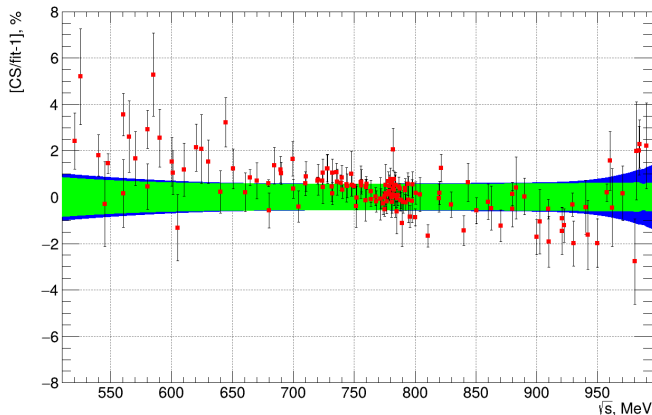
BaBar results deviation from our fit, green area – systematics, blue one - total uncertainty

$$a_\mu \times 10^{10} = 431.11 \pm 3.52 \text{ vs. BaBar: } a_\mu \times 10^{10} = 423.87 \pm 2.06$$





# Comparison with CMD-3 (UNBLINDED)



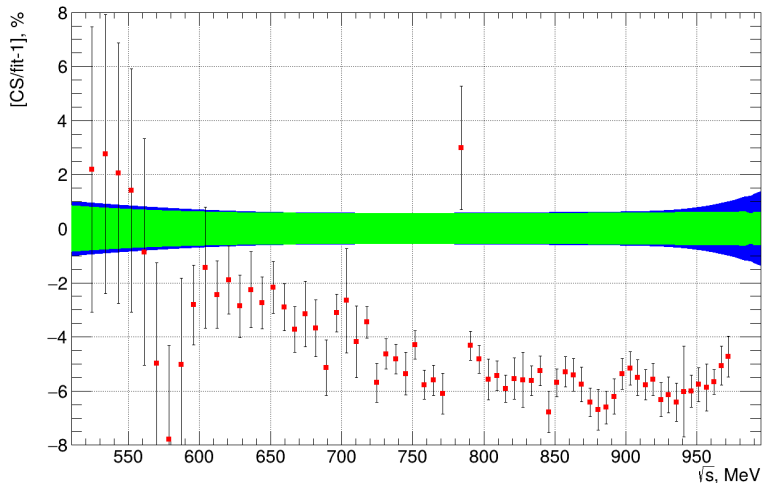
Deviation from our fit, green area – systematics, blue one - total uncertainty

$$a_\mu \times 10^{10} = 431.11 \pm 3.52 \text{ vs. CMD-3: } a_\mu \times 10^{10} = 433.62 \pm 3.76$$





# Comparison with KLOE (UNBLINDED)



Deviation from our fit, green area – systematics, blue one - total uncertainty





- We observe better agreement between the MC and Data efficiency
- Almost final (unblinded) result for the 2018 data is produced, with all corrections calculated
- Measurement of the cross section in  $520 \leq \sqrt{s} \leq 600$  MeV energy range with 2019 data using  $n=1.13$  ACC was performed, and it's consistent with 2018 data within 2%
- Application of the current analysis techniques to the 2013 data results in better agreement
- Calculated  $a_\mu$  is 1.7% ( $2\sigma$ ) higher than one derived from the BaBar data, and 0.6% lower comparing to the CMD-3 result





Thank you for attention !

